



Article

# Butyrate Decreases ICAM-1 Expression in Human Oral Squamous Cell Carcinoma Cells

Gabriel Leonardo Magrin <sup>1,2,†</sup> , Francesca Di Summa <sup>1,†</sup>, Franz-Josef Strauss <sup>1,3,4</sup> , Layla Panahipour <sup>1</sup> , Michael Mildner <sup>5</sup> , Cesar Augusto Magalhães Benfatti <sup>2</sup> and Reinhard Gruber <sup>1,6,\*</sup>

<sup>1</sup> Department of Oral Biology, School of Dentistry, Medical University of Vienna, Sensengasse 2a, Vienna 1090, Austria; gabriel.magrin@posgrad.ufsc.br (G.L.M.); francesca.disumma@studenti.unipr.it (F.D.S.); drstrauss@odontologia.uchile.cl (F.-J.S.); layla.panahipour@meduniwien.ac.at (L.P.)

<sup>2</sup> Center for Education and Research on Dental Implants (CEPID), Department of Dentistry, School of Dentistry, Federal University of Santa Catarina, Campus Reitor João David Ferreira Lima s/n, Florianópolis – SC 88040-900, Brazil; cesarbenfatti@yahoo.com

<sup>3</sup> Department of Conservative Dentistry, School of Dentistry, University of Chile, Av. Sergio Livingstone 943, Santiago 7500566, Chile

<sup>4</sup> Clinic of Reconstructive Dentistry, University of Zurich, 8032 Zurich, Switzerland

<sup>5</sup> Department of Dermatology, Medical University of Vienna, Spitalgasse 23, Vienna 1090, Austria; michael.mildner@meduniwien.ac.at

<sup>6</sup> Department of Periodontology, University Bern, Hochschulstrasse 4, 3012 Bern, Switzerland

\* Correspondence: reinhard.gruber@meduniwien.ac.at

† These authors contributed equally to this work.

Received: 3 January 2020; Accepted: 27 February 2020; Published: 29 February 2020



**Abstract:** Short-chain fatty acids (SCFA) are bacterial metabolites that can be found in periodontal pockets. The expression of adhesion molecules such as intercellular adhesion molecule-1 (ICAM-1) within the epithelium pocket is considered to be a key event for the selective transmigration of leucocytes towards the gingival sulcus. However, the impact of SCFA on ICAM-1 expression by oral epithelial cells remains unclear. We therefore exposed the oral squamous carcinoma cell line HSC-2, primary oral epithelial cells and human gingival fibroblasts to SCFA, namely acetate, propionate and butyrate, and stimulated with known inducers of ICAM-1 such as interleukin-1-beta (IL1 $\beta$ ) and tumor necrosis factor-alfa (TNF $\alpha$ ). We report here that butyrate but not acetate or propionate significantly suppressed the cytokine-induced ICAM-1 expression in HSC-2 epithelial cells and primary epithelial cells. The G-protein coupled receptor-43 (GPR43/FFAR2) agonist but not the histone deacetylase inhibitor, trichostatin A, mimicked the butyrate effects. Butyrate also attenuated the nuclear translocation of p65 into the nucleus on HSC-2 cells. The decrease of ICAM-1 was independent of Nrf2/HO-1 signaling and phosphorylation of JNK and p38. Nevertheless, butyrate could not reverse an ongoing cytokine-induced ICAM-1 expression in HSC-2 cells. Overall, these observations suggest that butyrate can attenuate cytokine-induced ICAM-1 expression in cells with epithelial origin.

**Keywords:** butyric acid; periodontium; intercellular adhesion molecule-1; oral biology; epithelial cells; in vitro

## 1. Introduction

Oral health requires the cellular immunity of the oral mucosal barrier that extends towards the periodontium to defend the tooth-bearing tissue against commensal microbes and other antigens of the oral cavity [1]. The junctional epithelium controls the transmigration of neutrophils towards the

crevicular fluid by means of a tightly controlled expression of adhesion molecules, thereby defending microbiological antagonism in the periodontal tissue [2,3]. Thus, the increase of adhesion molecules by inflammatory mediators has to be counterbalanced by local cues to control an excessive influx of cells of the innate immune system.

The influx of cells is controlled by intercellular adhesion molecule-1 (ICAM-1), allowing the transmigration of leucocytes which express the corresponding lymphocyte function-associated antigen-1 and macrophage adhesion ligand-1 [4]. ICAM-1, being induced by inflammatory cues such as interleukin-1-beta (IL1 $\beta$ ) and tumor necrosis factor- $\alpha$  (TNF $\alpha$ ) [5], is expressed by the vascular endothelium and by the junctional epithelium [6], thus, facilitating transmigration of leukocytes across vascular endothelia and the invasion of the extracellular matrix [7]. Although ICAM-1 is consistently expressed by junctional epithelial cells in healthy gingiva and in pocket epithelium, it is not detectable on the majority of keratinocytes in the external gingival epithelium [6,8]. The question then arises, how is the expression of ICAM-1 in epithelial cells controlled?

The increase of ICAM-1 expression by inflammatory cues is evidently well-documented. Inflammatory mediators including IL-6 and prostaglandin E<sub>2</sub> increase ICAM-1 expression in human oral squamous cell carcinoma SCC4 cells in vitro [9,10]. Primary gingival epithelial cells increasingly express ICAM-1 upon inflammatory cytokines stimuli, namely, TNF $\alpha$  and interferon- $\gamma$  [11]. Gingival fibroblasts also express ICAM-1 in response to inflammatory cytokines [12]. Nevertheless, the opposite effect, the down-regulation of ICAM-1, has not been conclusively defined. Down-regulation of ICAM-1 on bronchial epithelial cells has been observed with fenoterol, a  $\beta$ 2-adrenoceptor agonist [13], and in retinal pigment epithelial cells with bezafibrate, a drug to treat hyperlipidemia [14]. However, little is understood about what decreases ICAM-1 expression in oral epithelial cells.

Short-chain fatty acids (SCFA) are mainly produced by Gram-negative bacteria, being acetate, propionate, and butyrate the three most common molecules [15]. SCFA are found in the oral cavity, particularly in dental plaque and sites with periodontal disease [16,17]. Millimolar concentration of butyrate in the gingival crevicular fluid were correlated with gingival inflammation and periodontal pocket depth [18]. Anaerobic bacteria in subgingival plaques such as *Porphyromonas gingivalis*, *Treponema denticola*, *Aggregatibacter actinomycetemcomitans*, *Prevotella intermedia* and *Fusobacterium nucleatum* release SCFA, including butyrate [17]. Furthermore, butyrate from oral environment can cross the gingival barrier and potentially cause systemic inflammation and localized detrimental effects in the brain [19]. Taken together, it seems that butyrate and other SCFA are virulence factors in periodontal disease.

Butyrate can activate the free fatty acid receptor-2 (FFAR2), also known as G-protein coupled receptor-43 (GPR43) [20], but also inhibit the histone deacetylase (HDAC) [21]. Using either of these mechanisms, butyrate reduces proliferation and induces apoptosis in gingival fibroblast [22–25], stimulates T-cell apoptosis [26] and osteoblast maturation [27], as well as pro-inflammatory cytokine release by neutrophils [28]. Butyrate also reduced integrin expression in Ca9-22 epithelial cells [23,29] and promoted autophagy [30]. The presence of SCFA in the infectious site attenuates the neutrophils response to *A. actinomycetemcomitans* as a result of the inhibition of specific isoforms of HDACs, namely, HDAC 1 and 3, but not activation of FFAR2 [31]. Recent findings suggest that butyrate disturbs gingival epithelial homeostasis and initiates expression of pro-inflammatory cytokine in vitro [32]. Thus, there is accumulating evidence suggesting that SCFA has detrimental effects on cells of the periodontium. However, with respect to the beneficial effects of butyrate on colitis [33,34], pathological bone loss [35], anti-microbial activity [36], and on a M1-to-M2 shift in macrophages [37–39] it should not be ruled out that SCFA may also contribute to tissue homeostasis by modulation of ICAM-1.

Butyrate markedly reduces ICAM-1 expression in the intestine of severely burned rats [40] and in IL1 $\beta$ -stimulated chondrocytes [41]. Butyrate also reduces the expression of ICAM-1 in LPS-stimulated mouse glomerular mesangial and Caco-2 cells [42,43], and cytokine-induced ICAM-1 expression in cultured endothelial cells [44]. Conversely, other studies showed that butyrate increases ICAM-1 in human gingival carcinoma cell line Ca9-22 [23,45], in acute myeloid leukemia cells [46] and endothelial cells [47,48]. Owing to these inconsistent results, it cannot be predicted whether butyrate or other SCFA

change the expression of ICAM-1 in oral epithelia cells. The aim of this study was thus to investigate the influence of SCFA on the expression of ICAM-1 in oral cells with epithelial origin and to unravel possible underlying signaling pathways.

## 2. Results

### 2.1. Cell Viability Upon SCFA Stimulation at Varying Concentrations

In order to evaluate the impact of SCFA on cell viability, an MTT assay, reflecting the NAD(P)H-dependent formazan production, was carried out. To this end, HSC-2 and gingival fibroblasts were exposed to different concentration of SCFA ranging from 1 mM to 100 mM (Table 1). In case of acetate and propionate a concentration from 1 to 10 mM did not affect the viability of HSC-2 and gingival fibroblasts (Table 1). With respect to butyrate, a concentration up to 30 mM was tolerated by both cell types without altering their viability. Together, these observations indicate that 10 mM of SCFA is non-cytotoxic and therefore a suitable concentration for the following experiments.

**Table 1.** Cell viability of HSC-2 and gingival fibroblasts at varying concentrations of SCFA.

Cell Type	HSC-2 Cell Line			Gingival Fibroblasts		
	Concentration	Acetate	Propionate	Butyrate	Acetate	Propionate
100 mM	39.2 ± 5	46.4 ± 5.1	53.5 ± 5	12.5 ± 1.2	11.9 ± 1.5	10.1 ± 0.9
30 mM	45.8 ± 5.9	56.6 ± 5.8	95.8 ± 6	69.8 ± 4.5	74.5 ± 2.1	94 ± 0.5
10 mM	104.7 ± 6.1	113 ± 6.4	122.7 ± 6.5	96.3 ± 1.2	102.7 ± 1.2	122.3 ± 3.1
1 mM	125 ± 7.0	136 ± 5.6	139 ± 7.7	125.3 ± 6.7	130.4 ± 0.5	135.5 ± 6.5

HSC-2 cells and gingival fibroblasts exposed at different concentration of SCFA. Cell viability is represented by formazan production indicated in percentage of unstimulated controls ± SD. Cells maintained their viability with up to 10 mM of acetate and propionate, and up to 30 mM of butyrate.

### 2.2. Butyrate but Not Acetate and Propionate Decrease the Expression of ICAM-1 in HSC-2 Cells

Then, to examine the possible role of SCFA on ICAM-1 expression, the oral squamous cell carcinoma cell line HSC-2 and gingival fibroblasts were cultured for 12 h with and without acetate, propionate and butyrate. Subsequently, the cells were exposed for three hours to known inducers of ICAM-1, namely IL1 $\beta$  and TNF $\alpha$ . Butyrate exposure at 10 mM dampened down the robust cytokine-induced ICAM-1 mRNA expression in HSC-2 cells ( $p = 0.03$ ; Figure 1A) but not in gingival fibroblasts (Figure S1) or TR146 cells (Figure S2). In HSC-2 cells this suppression was dose-dependent (Figure 1B) and independent of the type of cytokine (Figure S3). Acetate and propionate at 10 mM, however, failed to cause a significant suppression of IL1 $\beta$ - and TNF $\alpha$ -induced ICAM-1 expression ( $p > 0.05$ , Figure 1A). Western blot analysis confirmed the marked suppression of ICAM-1 by butyrate (Figure 1C). Similarly, butyrate suppressed the cytokine-induced expression of ICAM-1 in primary oral epithelial cells (Figure 2). Then, and in order to validate these observations, we used another experimental setting using primary mouse macrophages [37–39]. Notably, butyrate was capable of inhibiting the LPS- and saliva-induced ICAM-1 expression in primary mouse macrophages (Figure 3). Collectively, these results suggest that butyrate suppresses the robust cytokine-induced ICAM-1 expression in HSC-2, primary oral epithelial cells and macrophages.

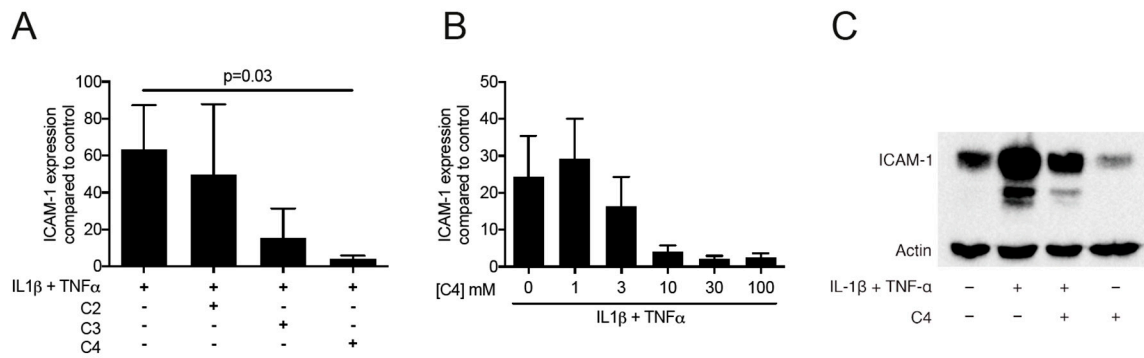


**Figure 1.** (A) Butyrate suppresses the cytokine-induced expression of ICAM-1 in HSC-2 cells. HSC-2 were exposed for 24 h to 10 mM of acetate (C2), propionate (C3) and butyrate (C4), and then stimulated for three hours with 10 ng/mL of IL1β and TNFα. (+), indicates presence; (-), indicates absence. Data represent the mean change of ICAM-1 expression ± standard deviation. *n* = 3. Statistical analysis was based on ANOVA test with Tukey’s multiple comparisons correction and significant *p*-values are indicated. (B) Butyrate suppresses the cytokine-induced increase of ICAM-1 in a dose-dependent manner. HSC-2 cells were exposed to different concentrations of butyrate in the presence of IL1β and TNFα. Data represent the mean change of ICAM-1 expression ± standard deviation. *n* = 3 (C) Butyrate attenuates the IL1β- and TNFα-induced expression of ICAM-1. HSC-2 cells were exposed to 10 mM of butyrate (C4) in the presence or absence of 10 ng/mL IL1β and TNFα.

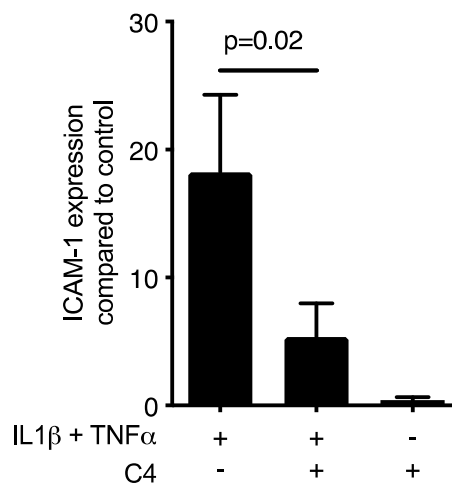


**Figure 2.** Butyrate suppresses the cytokine-induced increase of ICAM-1 in primary epithelial cells. Cells were exposed to 10 mM butyrate (C4) in the presence of 10 ng/mL IL1β and TNFα. (+), indicates presence; (-), indicates absence. Data represent the mean change of ICAM-1 expression ± standard deviation. *n* = 3. Statistical analysis was based on *t*-test and *p*-values are indicated.

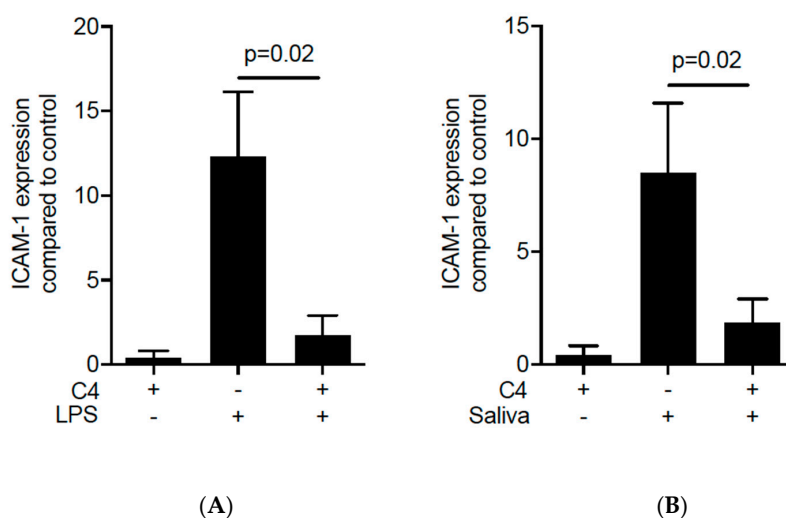


**Figure 3.** Butyrate suppresses the LPS- and saliva-induced increase of ICAM-1 in primary mouse macrophages. Cells were exposed to 10 mM of butyrate (C4) in the presence of (A) 100 ng/mL of LPS and (B) 2% saliva. (+), indicates presence; (-), indicates absence. Data represent the mean change of ICAM-1 expression  $\pm$  standard deviation.  $n = 4$ . Statistical analysis was based on Mann–Whitney U test and  $p$ -values are indicated.

### 2.3. Activation of FFAR2 Can Mimic the Activity of Butyrate on ICAM-1 in HSC-2 Cells

To distinguish between the dual activity of butyrate to activate the SCFA receptor FFAR2/GPR43 [20] from the histone deacetylase inhibition [21], HSC-2 cells were pre-exposed to a FFAR2/GPR43 agonist and to trichostatin A, an inhibitor of histone deacetylases. After 24 h of stimulation, IL1 $\beta$  and TNF $\alpha$  were added to induce ICAM-1. Similar to butyrate, the FFAR2/GPR43 agonist significantly reduced the cytokine-induced expression of ICAM-1 in HSC-2 cells (Figure 4). In contrast, trichostatin A failed to inhibit the ICAM-1 expression. Surprisingly, the FFAR2 agonist GLPG 0974 failed to reverse the effects of butyrate on ICAM-1 expression (data not shown). Overall, these observations partially suggest that the suppression activity of butyrate is due to an activation of FFARs rather than an inhibition of the histone deacetylase activity.

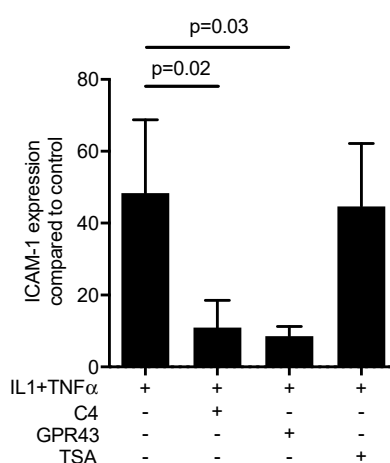


**Figure 4.** Activation of free fatty acid receptor-2 (FFAR2/GPR43) can mimic the activity of 10 mM of butyrate (C4) on ICAM-1 in HSC-2 cells. HSC-2 cells were exposed to a FFAR2/GPR43 agonist at 30  $\mu$ M and trichostatin A (TSA) at 10 nM, respectively, for 24 h before ICAM-1 was induced. (+), indicates presence; (-), indicates absence. Data represent the mean change of ICAM-1 expression  $\pm$  standard deviation.  $n = 3$ . Statistical analysis was based on Mann–Whitney U test and t-test,  $p$ -values are indicated.

#### 2.4. Butyrate Inhibits the Nuclear Translocation of p65 on HSC-2 cells

To explore a possible role of butyrate in inflammation, NF- $\kappa$ B p65 immunofluorescence was performed [49]. The presence of 10 mM of butyrate inhibited the IL1 $\beta$ - and TNF $\alpha$ -induced translocation of p65 protein into the nucleus in HSC-2 cells (Figure 5). Moreover, 10 mM of butyrate caused a 4-fold increase of  $\beta$ -arrestins-2 [50], known to be activated by FFAR2 receptor signaling, producing anti-inflammatory effects by inhibition of NF- $\kappa$ B [51,52]. This observation implies a suppression of the inflammatory activation by transcription factors triggered via NF- $\kappa$ B proteins that might involve Nrf2-HO1 signaling. However, blocking HO1 activity with SnPP failed to reverse the effects of butyrate on ICAM-1 expression in HSC2 cells (data not shown). Consistently, butyrate had no impact on HO-1 expression in HSC2 cells (data not shown) and the lack of Nrf2 had no impact on the suppression activity of butyrate on the LPS-induced ICAM-1 expression in primary macrophages (Figure S4). Since MAPK signaling cascade plays a key role in inflammation, we also examined the effect of butyrate on p38 and JNK expression to determine whether the suppressive activity of butyrate involves the MAPK pathway. Western blot analysis revealed that phosphorylation of p38 and JNK being involved in ICAM-1 expression, was not affected by the addition of butyrate (Figure S5). Taken together, these observations indicate that the ICAM-1-suppressive activity of butyrate is independent of Nrf2-HO1 and MAPK pathway.

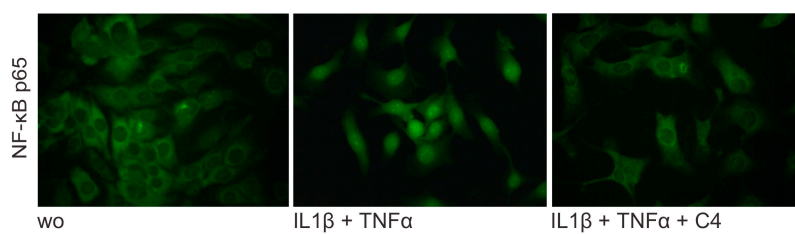


**Figure 5.** Butyrate suppresses NF- $\kappa$ B p65 translocation in inflamed HSC-2 cells. Butyrate at 10 mM attenuates the intracellular translocation of NF- $\kappa$ B p65 into the nucleus, induced by 10 ng/mL IL1 $\beta$  and TNF $\alpha$  in HSC-2. (wo), without. Representative immunofluorescence at 40x.

#### 2.5. Butyrate Cannot Reverse the Acute Expression Levels of ICAM-1 in HSC-2 Cells

In the previous experimental setting, HSC-2 cells were exposed to butyrate for 24 h, before the incubation with IL1 $\beta$  and TNF $\alpha$ , simulating a prophylactic effect of butyrate. To investigate the possible role of butyrate in dampening the acute ICAM-1 expression, HSC-2 cells were exposed to IL1 $\beta$  and TNF $\alpha$  for 1 h and then butyrate was added for another 3 h. In this setting, butyrate failed to modulate the ICAM-1 expression in HSC-2 cells suggesting that butyrate can prevent but not reverse an ongoing ICAM-1 expression in inflammatory conditions (Figure 6). Moreover, three hours of pre-exposure of HSC-2 cells with butyrate also failed to reduce the IL1 $\beta$  and TNF $\alpha$ -induced increase of ICAM-1, suggesting that a longer period of pre-incubation with butyrate is critical to obtain aICAM-1 modulation [53].

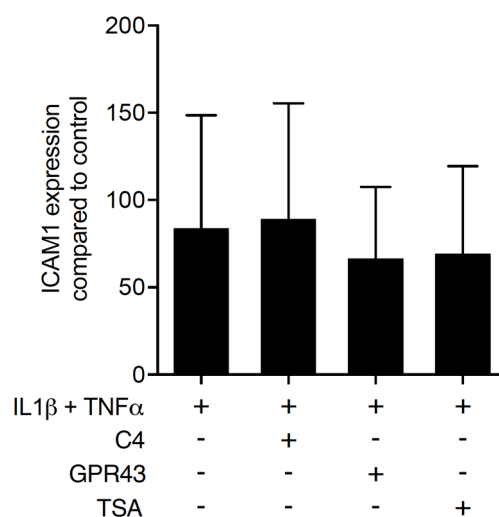


**Figure 6.** Butyrate cannot reverse expression levels of ICAM-1 in HSC-2 cells. HSC-2 cells were exposed to 10 ng/mL IL1 $\beta$  and TNF $\alpha$  for 1 h before 10 mM of butyrate (C4) was added for another 3 h. In this setting, butyrate FFAR2/GPR43 agonist and trichostatin A (TSA) failed to modulate the ICAM-1 expression in HSC-2 cells. (+), indicates presence; (-), indicates absence. Data represent the mean change of ICAM-1 expression  $\pm$  standard deviation.  $n = 3$ . Statistical analysis was based on *t*-test.

### 3. Discussion

Our findings showed that butyrate but not acetate or propionate attenuates the cytokine-induced ICAM-1 expression in oral squamous cells. This effect was consistent in all experiments performed, being confirmed at the transcriptional and the protein levels. The changes of ICAM-1 expression were further confirmed with primary oral epithelial cells and macrophages, while gingival fibroblasts failed to respond to butyrate. These observations raise the hypothesis that butyrate can modulate epithelial cell responses in the inflamed periodontium and thereby possibly influencing the ICAM-1-dependent transmigration of leucocytes and immune cells. It seems reasonable to relate the production of butyrate by periodontal pathogens with the severity of periodontitis. In this sense, a possible mechanism might be that the reduction of ICAM-1 expression lowers the influx of leukocytes to the inflamed tissue thereby hampering the immune system to tackle bacterial invasion. Nevertheless, further research is required to elucidate the precise role of butyrate in the periodontal tissues under different *in vitro* conditions.

Our research supports the role of butyrate to reduce ICAM-1 expression as observed in the intestine of burned rats [40], stimulated chondrocytes [41], glomerular mesangial cells [42], colon cancer cells [43], and endothelial cells [44]. These observations together with our findings are, however, in contrast to those showing that butyrate increases ICAM-1 in gingival carcinoma cells [23,45], leukemia cells [46] and endothelial cells [47,48]. Furthermore, high concentrations of butyrate provoke apoptosis in inflamed human gingival fibroblasts and periodontal destruction [25,29]. The testing of acetate and propionate was also hampered by the higher toxicity compared to butyrate. Surprising was that although acetate and propionate are agonist for the FFAR2/GPR43, only butyrate caused the robust and significant suppression of ICAM-1 expression [52]. Moreover, blocking of FFAR2/GPR43 by the antagonist GLPG 0974 failed to reverse the effects of butyrate on ICAM-1 expression. This raises the question whether the FFAR3/GPR41 is mediating the activity of butyrate [54]. Thus, further research is necessary to unravel the underlying mechanism at the receptor level.

The FFAR2 receptor activates  $\beta$ -arrestins-2, producing anti-inflammatory effects by inhibition of NF- $\kappa$ B [51,52] and ICAM-1 has a NF $\kappa$ B binding promoter region [55]. In support of this potential mechanism, we show that  $\beta$ -arrestins-2 is increased by butyrate in HSC-2 cells. Hence, the blocking of NF $\kappa$ B nuclear translocation likely reduces ICAM-1 expression, being in line with our main observations on the regulation of ICAM-1 by butyrate. The reason why TR146 cells and gingival fibroblasts failed

to respond to butyrate may be explained by their low increase of ICAM-1 expression in response to inflammatory cytokines. However, also short-time exposure of HSC-2 cells to butyrate had no considerable effect suggesting that not enough  $\beta$ -arrestins-2 is produced to reduce NF- $\kappa$ B signaling. Certainly, the role of butyrate to change  $\beta$ -arrestins-2 expression and the involvement in ICAM-1 expression in HSC-2 cells should be investigated. Although many questions remain open, the present data clearly show that butyrate can prevent the cytokine-induced ICAM-1 expression in oral squamous cell carcinoma cells, primary oral epithelial cells and macrophages.

To better understand the underlying molecular mechanisms, the Nrf2-HO1 pathway was investigated. Butyrate uses the Nrf2/HO-1 pathway to ameliorate diabetic nephropathy [56], to regulate Th17/Treg cell balance [57] and to protect against high-fat diet-induced oxidative stress in rat liver [58]. There is also evidence that butyrate inhibits the acute lung injury in mice by regulating the NF $\kappa$ B signaling pathway [59]. Moreover, Nrf2-HO1 signaling is linked to ICAM-1 expression in a mouse atherosclerosis model [60], in THP-1 macrophages [61], and HaCaT cells [62]. However, in the present study, SnPP blocking HO1 activity could not reverse the inhibition of butyrate in ICAM-1 expression. Indeed, macrophages from Nrf2 knockout and wildtype mice showed similar inhibition of ICAM-1 expression. Even though Nrf2-HO1 signaling was a strong candidate to mediate the effects of butyrate, this mechanism is presumably not relevant for the observations we have reported here. Furthermore, butyrate failed to reduce the phosphorylation of p38 and JNK, both major signaling molecules driving NF $\kappa$ B signaling and ICAM-1 expression in HSC-2 cells suggesting that other pathways than Nrf2-HO1 and MAPK signaling are relevant to explain the strong inhibition of ICAM-1 by butyrate [62–64].

Are the present findings clinically relevant? To answer that question, it is worth mentioning that the commensal bacteria that induce a low-grade inflammatory state in the junctional epithelium are likely the triggers of ICAM-1 expression and neutrophil migration [7]. Thus, there is strong ICAM-1 staining of the junctional epithelium in both clinically healthy and inflamed tissue [2], even though soluble ICAM-1 shed into the gingival crevicular fluid was higher in patients with inflammation [63]. Considering that mice deficient in ICAM-1 have impaired immune function and decreased inflammatory response [64], a decrease of ICAM-1 in epithelial cells caused by butyrate might weaken the innate immunity and thus the local defense of the periodontium. Regarding the role of ICAM-1 in macrophages, this also remains controversial. ICAM-1 deficiency increases M2 macrophage polarization and suppresses tumor metastasis [65], but others reported that downregulation of ICAM-1 in RAW264.7 macrophages resulted in inflammatory M1 polarization [66]. Therefore, the possible implication of ICAM-1 expression in macrophages and its regulation by butyrate in periodontal tissue homeostasis remains to be determined.

This study has limitations that need to be acknowledged. Our finding that butyrate protects cells from cytokine-induced ICAM-1 expression in oral squamous cell carcinoma cells *in vitro* does not necessarily explain the *in vivo* situation. Notably, butyrate failed to diminish an ongoing ICAM-1 expression in HSC-2 cells. It would be interesting to determine the impact of SCFA on periodontitis by means of *in vivo* models. For example, it can be suggested to study the role of epithelial ICAM-1 on healthy periodontium, the impact of the SCFA receptors in this context, and whether butyrate produced by periodontal pathogens plays a role in pathogenesis of periodontitis. Furthermore, exciting questions about how SCFA from non-digestible nutritional fibers metabolized by gut bacteria [67] can enter the bloodstream and elicit systemic effects should be addressed. An optimized diet rich in fibers can reduce gingival and periodontal inflammation in humans [68,69]. This observation inspires further research towards a possible beneficial role of butyrate on ICAM-1 expression in the periodontal tissue. Moreover, future studies should be performed in FFAR2 and FFAR3-deficient mice asking if butyrate can prevent inflammatory osteolysis [70,71], and if yes, if this effect also involves the blocking of the histone deacetylase [72,73].

In conclusion, our findings that butyrate modulates the inflammatory response in oral epithelial cells by decreasing ICAM-1 expression provide a new step towards understanding the effect of ICAM-1



under inflammatory conditions. These *in vitro* data may inspire future research on the mechanisms by which diet, microbiota and other factors influence the immune system and, consequently, the development of inflammatory and infectious diseases.

## 4. Material and Methods

### 4.1. Cell Culture

Human oral epithelial carcinoma cells HSC-2 and TR146 were kindly provided by Prof. Rausch-Fan from Medical University of Vienna, Vienna, Austria. Gingival fibroblasts and primary epithelial cells were obtained from human gingiva harvested from extracted third molars of patients who had given informed and written consent. Gingival fibroblasts were prepared by explant cultures. The epithelium was separated from the underlying connective tissue after overnight dispase II (2.4 U/mL; Roche, Mannheim, Germany) treatment, and preparation of single-cell suspension by means of trypsin (Lonza, Walkersville, MD) digestion at 37 °C for 10 min. Epithelial cells were expanded in growth medium-2 (KGM-2; Lonza, Basel, Switzerland). The Ethics Committee of the Medical University of Vienna (EK NR 631/2007, 19 March 2019) Vienna, Austria, approved this protocol. Cell lines and gingival fibroblasts were cultured in Dulbecco's modified Eagle medium (DMEM, Invitrogen Corporation, Carlsbad, CA, USA) supplemented with 10% fetal calf serum (Invitrogen Corporation, Carlsbad, CA, USA) and antibiotics (Invitrogen Corporation, Carlsbad, CA, USA) at 37 °C, 5% CO<sub>2</sub>, and 95% humidity. Gingival epithelial cells were cultured in keratinocyte growth medium-2 (KGM-2; Lonza, Basel, Switzerland) at 37 °C, 5% CO<sub>2</sub>, and at 95% relative humidity. Cells were seeded in growth medium at a concentration of at least 30,000 cells/cm<sup>2</sup> onto culture dishes one day prior to stimulation. Serum-free conditions were used during cell stimulation. For the isolation and culture of murine bone marrow-derived macrophages, BALB/c mice (Animal Research Laboratories, Himberg, Austria) of 6–8 weeks old were purchased. Bone marrow cells were collected from the femora and tibiae and grown for 5 days in Minimum Essential Medium Eagle-Alpha Modification (αMEM, Invitrogen Corporation, Carlsbad, CA, USA), supplemented with 10% fetal calf serum and antibiotics, supplemented with 20 ng/mL macrophage colony-stimulating factor (M-CSF; ProSpec-Tany TechnoGene Ltd., Rehovot, Israel). For selected experiments, cells from Nrf2 knockout mice and the respective wildtype controls were used (Prof. Florian Gruber, Department of Dermatology, Medical University of Vienna, Vienna, Austria).

### 4.2. Viability Assay

Epithelial HSC-2 cells and gingival fibroblasts were incubated with different concentrations of acetate, propionate and butyrate (Sigma-Aldrich, St. Louis, MO, USA) or serum-free medium in 96-well plates (CytoOne, Starlab International, Hamburg, Germany). After 24 h, a final concentration of 0.5 mg/mL of a MTT - 3-(4,5-dimethylthiazol-2-yl)-2,5-diphenyltetrazolium bromide – (Sigma-Aldrich, St. Louis, MO, USA) solution was added to each well of the microtiter plate for 3 h at 37 °C. After medium removal, formazan crystals were solubilized with dimethyl sulfoxide. Assessment of optical density was carried out for 570 nm. Absolute numbers of optical density in the treatment groups were expressed and presented as percentage of unstimulated controls ± standard deviation.

### 4.3. Cell Stimulation

Based on the findings from the viability assay, stimulation of HSC-2 cells and gingival fibroblasts was performed with 10 mM of acetate, propionate and butyrate. As a basic setting for the experiments, cells were exposed to SCFA for 24 h in serum-free medium before the addition of 10 ng/mL IL1β and TNFα (ProSpec-Tany TechnoGene Ltd., Rehovot, Israel) for another three hours, after that gene expression analysis of ICAM-1 was performed. Likewise, the oral squamous cell carcinoma cell line TR146 was exposed to butyrate in the same conditions of HSC-2. Macrophages were exposed to SCFA for 24 h in growth medium before the addition of LPS (100 ng/mL, LPS from *Escherichia coli* 0111: B4; Sigma-Aldrich, St. Louis, MO, USA) or 2% of sterile pooled human saliva [74] for another three hours.

For dose-response experiments in HSC-2 cells, concentrations of 1, 10, 30 and 100 mM of butyrate were used. HSC-2 cells were further exposed to GPR43 (FFAR2) agonist (Merck KGaA, Darmstadt, Germany) at 30  $\mu$ M and the histone deacetylase inhibitor trichostatin A at 10 nM (Sigma-Aldrich, St. Louis, MO, USA) for 24 h before inflammation was induced accordingly. In another series of experiments, HSC-2 cells were exposed to IL1 $\beta$  and TNF $\alpha$  for 1 h followed by the exposure to 10 mM butyrate for three hours, or exposed to butyrate either alone or in the presence of tin protoporphyrin IX dichloride (SnPP; Sigma-Aldrich, St. Louis, MO, USA) at a concentration of 10  $\mu$ M. We have included a rescue experiment by using the inhibitor of FFAR2 named GLPG 0974 at 10  $\mu$ M (Tocris Bioscience™, Abingdon, UK).

#### 4.4. qRT-PCR Analysis

ExtractMe total RNA kit (Blirt S.A., Gdańsk, Poland) was used for RNA isolation. Reverse transcription was then performed by means of SensiFAST™ cDNA (Bioline, London, UK). For polymerase chain reaction, SensiFAST™ SYBR ROX Kit (Bioline, London, UK) on a Real-Time PCR Detection System (Bio-Rad Laboratories, Hercules, CA, USA) was carried out. Primer sequences used are described in Table 2. The mRNA levels were calculated by normalizing to the housekeeping gene GAPDH using the  $\Delta\Delta$ Ct method.

**Table 2.** Primer sequences.

Primer	Sequence Forward	Sequence Reverse
hICAM-1	cct tcc tca ceg tgt act gg	agc gta ggg taa ggt tct tgc
hARRB2	caa ctc cac caa gac cgt caa ga	ttc gag ttg agc cac agg aca ctt
hGAPDH	aag cca cat cgc tca gac ac	gcc caa tac gac caa atc c
hActin	cca acc gcg aga aga tga	cca gag gcg tac agg gat ag
mICAM-1	gtg atg ctc agg tat cca tcc a	cac agt tct caa agc aca gcg
mGAPDH	aac ttt ggc att gtg gaa gg	gga tgc agg gat gat gtt ct
mActin	cta agg cca acc gtg aaa ag	acc aga ggc ata cag gga ca

#### 4.5. Western Blot

After stimulation with butyrate for 24 h and the inflammatory cytokines IL1 $\beta$  and TNF $\alpha$  for another three hours, HSC-2 cells were extracted with SDS buffer and inhibitors of protease (PhosSTOP with cOmplete; Sigma-Aldrich, St. Louis, MO, USA), divided by SDS-PAGE and transferred onto nitrocellulose membranes (Whatman, GE Healthcare, General Electric Company, Fairfield, CT, USA). Thereafter, membranes were submitted to blocking process for 2 h and exposed to the first antibodies (mouse ICAM-1 G-5 and actin C-2 both at 200 ng/mL; Santa Cruz Biotechnology, Santa Cruz, CA, USA) for 24 h. In another series, HSC-2 cells were exposed to butyrate for 24 h and to the cytokines for 30 min before exposed to antibodies against phosphorylated and complete p38 and c-Jun N terminal protein kinase MAPK (both Cell Signaling Technologies, Danvers, MA, USA). Then, proteins were detected by the appropriate HRP-conjugated secondary antibody at 40 ng/mL (Santa Cruz Biotechnology, Santa Cruz, CA, USA). Subsequently, chemiluminescence detection (Clarity ECL Western Blot Substrate kit, Bio-Rad Laboratories, Hercules, CA, USA) was performed with a ChemiDoc MP System (Bio-Rad Laboratories, Hercules, CA, USA).

#### 4.6. Immunofluorescence

Immunofluorescent analysis was performed on HSC-2 cells plated onto Millicell® EZ slides (Merck KGaA, Darmstadt, Germany) treated with 10 mM of butyrate overnight and then exposed to IL1 $\beta$  and TNF $\alpha$  for 30 min. Cells were fixed in 4% paraformaldehyde and blocked in 1% BSA and 0.1% Triton in buffered saline before being incubated with nuclear factor kappa B (NF- $\kappa$ B) p65 antibody (25 ng/mL, rabbit, Cell Signaling Technology, MA, USA) overnight at 4 °C. After washing, Alexa Fluor 488 secondary antibody (4  $\mu$ g/mL; anti-rabbit, Cell Signaling Technology, MA, USA) was applied for

1 h at room temperature. Glass slides were mounted and images were captured at 40x under a Zeiss Axiovert 200 M fluorescent microscope (Carl Zeiss AG, Oberkochen, Germany).

#### 4.7. Statistical Analysis

All experiments were repeated at least three times. Bars show the mean and standard deviation of the data from all independent experiments. Normality of the data was assessed using the Shapiro-Wilk test. Statistical analysis was based on t-test and ANOVA or Mann–Whitney U test depending on the distribution of the data. Analyses were performed using Prism v7 (GraphPad Software, La Jolla, CA, USA). Significance was set at  $p < 0.05$ .

**Supplementary Materials:** Supplementary materials can be found at <http://www.mdpi.com/1422-0067/21/5/1679/s1>.

**Author Contributions:** Conceptualization, R.G.; Data curation, G.L.M., F.D.S. and L.P.; Formal analysis, F.D.S. and L.P.; Funding acquisition, F.-J.S. and R.G.; Methodology, G.L.M., F.D.S. and M.M.; Project administration, R.G.; Resources, M.M.; Software, L.P.; Supervision, F.-J.S. and C.A.M.B.; Validation, L.P.; Visualization, F.D.S. and L.P.; Writing—original draft, G.L.M. and R.G.; Writing—review & editing, F.-J.S., M.M. and R.G. All authors have read and agreed to the published version of the manuscript.

**Funding:** This research was supported by a grant from Austrian Science Fund (FWF) (4072-B28). Gabriel Leonardo Magrin is supported by a scholarship from the Coordination for Improvement of Higher Education Personnel (CAPES), Brazil. Franz Josef Strauss is supported by a grant (17-125) from the Osteology Foundation, Switzerland, and the Comisión Nacional de Investigación Científica y Tecnológica (CONICYT), Chile. The authors declare that they have no conflict of interest.

**Acknowledgments:** The authors would like to thank Martina Wiederstein for technical support. The authors also thank Rami Rasho and Anna Somweber for collecting preliminary data for this research and Jila Nasirzade and Zhara Kargarpour for their technical and scientific contributions during the experimental phase of this study. Rausch-Fan from Medical University of Vienna kindly provided human oral epithelial carcinoma cells HSC-2 and TR146 for our experiments. The authors acknowledge the Austrian Science Fund (FWF) for the Open Access Funding.

**Conflicts of Interest:** The authors declare no conflict of interest. The funders had no role in the design, execution, interpretation, or writing of the study.

#### References

1. Mombelli, A. Microbial colonization of the periodontal pocket and its significance for periodontal therapy. *Periodontol 2000* **2018**, *76*, 85–96. [[CrossRef](#)]
2. Moughal, N.A.; Adonogianaki, E.; Thornhill, M.H.; Kinane, D.F. Endothelial cell leukocyte adhesion molecule-1 (ELAM-1) and intercellular adhesion molecule-1 (ICAM-1) expression in gingival tissue during health and experimentally-induced gingivitis. *J. Periodontal Res.* **1992**, *27*, 623–630. [[CrossRef](#)] [[PubMed](#)]
3. Tsuchida, S.; Satoh, M.; Takiwaki, M.; Nomura, F. Current Status of Proteomic Technologies for Discovering and Identifying Gingival Crevicular Fluid Biomarkers for Periodontal Disease. *Int. J. Mol. Sci.* **2018**, *20*, 86. [[CrossRef](#)] [[PubMed](#)]
4. Blanks, J.E.; Moll, T.; Eytner, R.; Vestweber, D. Stimulation of P-selectin glycoprotein ligand-1 on mouse neutrophils activates beta 2-integrin mediated cell attachment to ICAM-1. *Eur J. Immunol* **1998**, *28*, 433–443. [[CrossRef](#)]
5. Rothlein, R.; Czajkowski, M.; O'Neill, M.M.; Marlin, S.D.; Mainolfi, E.; Merluzzi, V.J. Induction of intercellular adhesion molecule 1 on primary and continuous cell lines by pro-inflammatory cytokines. Regulation by pharmacologic agents and neutralizing antibodies. *J. Immunol.* **1988**, *141*, 1665–1669.
6. Crawford, J.M.; Hopp, B. Junctional epithelium expresses the intercellular adhesion molecule ICAM-1. *J. Periodontal Res.* **1990**, *25*, 254–256. [[CrossRef](#)]
7. Irie, K.; Tomofuji, T.; Ekuni, D.; Morita, M.; Shimazaki, Y.; Darveau, R.P. Impact of Oral Commensal Bacteria on Degradation of Periodontal Connective Tissue in Mice. *J. Periodontol.* **2015**, *86*, 899–905. [[CrossRef](#)]
8. Crawford, J.M. Distribution of ICAM-1, LFA-3 and HLA-DR in healthy and diseased gingival tissues. *J. Periodontal Res.* **1992**, *27*, 291–298. [[CrossRef](#)]

9. Yang, S.F.; Chen, M.K.; Hsieh, Y.S.; Chung, T.T.; Hsieh, Y.H.; Lin, C.W.; Su, J.L.; Tsai, M.H.; Tang, C.H. Prostaglandin E2/EP1 signaling pathway enhances intercellular adhesion molecule 1 (ICAM-1) expression and cell motility in oral cancer cells. *J. Biol. Chem.* **2010**, *285*, 29808–29816. [[CrossRef](#)]
10. Chuang, J.Y.; Huang, Y.L.; Yen, W.L.; Chiang, I.P.; Tsai, M.H.; Tang, C.H. Syk/JNK/AP-1 signaling pathway mediates interleukin-6-promoted cell migration in oral squamous cell carcinoma. *Int. J. Mol. Sci.* **2014**, *15*, 545–559. [[CrossRef](#)]
11. Huang, G.T.; Haake, S.K.; Kim, J.W.; Park, N.H. Differential expression of interleukin-8 and intercellular adhesion molecule-1 by human gingival epithelial cells in response to *Actinobacillus actinomycetemcomitans* or *Porphyromonas gingivalis* infection. *Oral. Microbiol. Immunol.* **1998**, *13*, 301–309. [[CrossRef](#)] [[PubMed](#)]
12. Takahashi, K.; Takigawa, M.; Takashiba, S.; Nagai, A.; Miyamoto, M.; Kurihara, H.; Murayama, Y. Role of cytokine in the induction of adhesion molecules on cultured human gingival fibroblasts. *J. Periodontol.* **1994**, *65*, 230–235. [[CrossRef](#)] [[PubMed](#)]
13. Oddera, S.; Silvestri, M.; Lantero, S.; Sacco, O.; Rossi, G.A. Downregulation of the expression of intercellular adhesion molecule (ICAM)-1 on bronchial epithelial cells by fenoterol, a beta2-adrenoceptor agonist. *J. Asthma* **1998**, *35*, 401–408. [[CrossRef](#)]
14. Usui-Ouchi, A.; Ouchi, Y.; Ebihara, N. The peroxisome proliferator-activated receptor pan-agonist bezafibrate suppresses microvascular inflammatory responses of retinal endothelial cells and vascular endothelial growth factor production in retinal pigmented epithelial cells. *Int. Immunopharmacol.* **2017**, *52*, 70–76. [[CrossRef](#)] [[PubMed](#)]
15. Macfarlane, G.T.; Macfarlane, S. Bacteria, colonic fermentation, and gastrointestinal health. *J. AOAC Int* **2012**, *95*, 50–60. [[CrossRef](#)] [[PubMed](#)]
16. Singer, R.E.; Buckner, B.A. Butyrate and propionate: Important components of toxic dental plaque extracts. *Infect. Immun.* **1981**, *32*, 458–463. [[CrossRef](#)] [[PubMed](#)]
17. Lu, R.; Meng, H.; Gao, X.; Xu, L.; Feng, X. Effect of non-surgical periodontal treatment on short chain fatty acid levels in gingival crevicular fluid of patients with generalized aggressive periodontitis. *J. Periodontal Res.* **2014**, *49*, 574–583. [[CrossRef](#)]
18. Niederman, R.; Buyle-Bodin, Y.; Lu, B.Y.; Robinson, P.; Naleway, C. Short-chain carboxylic acid concentration in human gingival crevicular fluid. *J. Dent. Res.* **1997**, *76*, 575–579. [[CrossRef](#)]
19. Cueno, M.E.; Ochiai, K. Gingival Periodontal Disease (PD) Level-Butyric Acid Affects the Systemic Blood and Brain Organ: Insights Into the Systemic Inflammation of Periodontal Disease. *Front. Immunol.* **2018**, *9*, 1158. [[CrossRef](#)]
20. Kimura, I.; Ichimura, A.; Ohue-Kitano, R.; Igarashi, M. Free Fatty Acid Receptors in Health and Disease. *Physiol. Rev.* **2019**. [[CrossRef](#)]
21. Davie, J.R. Inhibition of histone deacetylase activity by butyrate. *J. Nutr* **2003**, *133*, 2485S–2493S. [[CrossRef](#)] [[PubMed](#)]
22. Jeng, J.H.; Chan, C.P.; Ho, Y.S.; Lan, W.H.; Hsieh, C.C.; Chang, M.C. Effects of butyrate and propionate on the adhesion, growth, cell cycle kinetics, and protein synthesis of cultured human gingival fibroblasts. *J. Periodontol.* **1999**, *70*, 1435–1442. [[CrossRef](#)] [[PubMed](#)]
23. Takigawa, S.; Sugano, N.; Nishihara, R.; Koshi, R.; Murai, M.; Yoshinuma, N.; Ochiai, K.; Ito, K. The effect of butyric acid on adhesion molecule expression by human gingival epithelial cells. *J. Periodontal Res.* **2008**, *43*, 386–390. [[CrossRef](#)] [[PubMed](#)]
24. Kurita-Ochiai, T.; Seto, S.; Suzuki, N.; Yamamoto, M.; Otsuka, K.; Abe, K.; Ochiai, K. Butyric acid induces apoptosis in inflamed fibroblasts. *J. Dent. Res.* **2008**, *87*, 51–55. [[CrossRef](#)] [[PubMed](#)]
25. Shirasugi, M.; Nishioka, K.; Yamamoto, T.; Nakaya, T.; Kanamura, N. Normal human gingival fibroblasts undergo cytoarrest and apoptosis after long-term exposure to butyric acid. *Biochem. Biophys. Res. Commun.* **2017**, *482*, 1122–1128. [[CrossRef](#)]
26. Kurita-Ochiai, T.; Fukushima, K.; Ochiai, K. Butyric acid-induced apoptosis of murine thymocytes, splenic T cells, and human Jurkat T cells. *Infect. Immun.* **1997**, *65*, 35–41. [[CrossRef](#)]
27. Schroeder, T.M.; Westendorf, J.J. Histone deacetylase inhibitors promote osteoblast maturation. *J. Bone Miner. Res.* **2005**, *20*, 2254–2263. [[CrossRef](#)]
28. Niederman, R.; Zhang, J.; Kashket, S. Short-chain carboxylic-acid-stimulated, PMN-mediated gingival inflammation. *Crit. Rev. Oral. Biol. Med.* **1997**, *8*, 269–290. [[CrossRef](#)]

29. Tsuda, H.; Ochiai, K.; Suzuki, N.; Otsuka, K. Butyrate, a bacterial metabolite, induces apoptosis and autophagic cell death in gingival epithelial cells. *J. Periodontol Res.* **2010**, *45*, 626–634. [[CrossRef](#)]
30. Evans, M.; Murofushi, T.; Tsuda, H.; Mikami, Y.; Zhao, N.; Ochiai, K.; Kurita-Ochiai, T.; Yamamoto, M.; Otsuka, K.; Suzuki, N. Combined effects of starvation and butyrate on autophagy-dependent gingival epithelial cell death. *J. Periodontol Res.* **2017**, *52*, 522–531. [[CrossRef](#)]
31. Correa, R.O.; Vieira, A.; Sernaglia, E.M.; Lancellotti, M.; Vieira, A.T.; Avila-Campos, M.J.; Rodrigues, H.G.; Vinolo, M.A.R. Bacterial short-chain fatty acid metabolites modulate the inflammatory response against infectious bacteria. *Cell Microbiol.* **2017**, *19*, e12720. [[CrossRef](#)] [[PubMed](#)]
32. Liu, J.; Wang, Y.; Meng, H.; Yu, J.; Lu, H.; Li, W.; Lu, R.; Zhao, Y.; Li, Q.; Su, L. Butyrate rather than LPS subverts gingival epithelial homeostasis by downregulation of intercellular junctions and triggering pyroptosis. *J. Clin. Periodontol.* **2019**, *46*, 894–907. [[CrossRef](#)] [[PubMed](#)]
33. Di Sabatino, A.; Morera, R.; Ciccocioppo, R.; Cazzola, P.; Gotti, S.; Tinozzi, F.P.; Tinozzi, S.; Corazza, G.R. Oral butyrate for mildly to moderately active Crohn’s disease. *Aliment. Pharmacol. Ther.* **2005**, *22*, 789–794. [[CrossRef](#)] [[PubMed](#)]
34. Butzner, J.D.; Parmar, R.; Bell, C.J.; Dalal, V. Butyrate enema therapy stimulates mucosal repair in experimental colitis in the rat. *Gut* **1996**, *38*, 568–573. [[CrossRef](#)] [[PubMed](#)]
35. Lucas, S.; Omata, Y.; Hofmann, J.; Bottcher, M.; Iljazovic, A.; Sarter, K.; Albrecht, O.; Schulz, O.; Krishnacoumar, B.; Kronke, G.; et al. Short-chain fatty acids regulate systemic bone mass and protect from pathological bone loss. *Nat. Commun.* **2018**, *9*, 55. [[CrossRef](#)]
36. Schulthess, J.; Pandey, S.; Capitani, M.; Rue-Albrecht, K.C.; Arnold, I.; Franchini, F.; Chomka, A.; Ilott, N.E.; Johnston, D.G.W.; Pires, E.; et al. The Short Chain Fatty Acid Butyrate Imprints an Antimicrobial Program in Macrophages. *Immunity* **2019**, *50*, 432–445. [[CrossRef](#)] [[PubMed](#)]
37. Ji, J.; Shu, D.; Zheng, M.; Wang, J.; Luo, C.; Wang, Y.; Guo, F.; Zou, X.; Lv, X.; Li, Y.; et al. Microbial metabolite butyrate facilitates M2 macrophage polarization and function. *Sci. Rep.* **2016**, *6*, 24838. [[CrossRef](#)]
38. Lee, C.; Kim, B.G.; Kim, J.H.; Chun, J.; Im, J.P.; Kim, J.S. Sodium butyrate inhibits the NF-kappa B signaling pathway and histone deacetylation, and attenuates experimental colitis in an IL-10 independent manner. *Int. Immunopharmacol.* **2017**, *51*, 47–56. [[CrossRef](#)]
39. Chen, G.; Ran, X.; Li, B.; Li, Y.; He, D.; Huang, B.; Fu, S.; Liu, J.; Wang, W. Sodium Butyrate Inhibits Inflammation and Maintains Epithelium Barrier Integrity in a TNBS-induced Inflammatory Bowel Disease Mice Model. *EBioMedicine* **2018**, *30*, 317–325. [[CrossRef](#)]
40. Liu, S.; Chen, H.Z.; Xu, Z.D.; Wang, F.; Fang, H.; Bellanfante, O.; Chen, X.L. Sodium butyrate inhibits the production of HMGB1 and attenuates severe burn plus delayed resuscitation-induced intestine injury via the p38 signaling pathway. *Burns* **2018**. [[CrossRef](#)]
41. Pirozzi, C.; Francisco, V.; Guida, F.D.; Gomez, R.; Lago, F.; Pino, J.; Meli, R.; Gualillo, O. Butyrate Modulates Inflammation in Chondrocytes via GPR43 Receptor. *Cell Physiol. Biochem.* **2018**, *51*, 228–243. [[CrossRef](#)] [[PubMed](#)]
42. Huang, W.; Guo, H.L.; Deng, X.; Zhu, T.T.; Xiong, J.F.; Xu, Y.H.; Xu, Y. Short-Chain Fatty Acids Inhibit Oxidative Stress and Inflammation in Mesangial Cells Induced by High Glucose and Lipopolysaccharide. *Exp. Clin. Endocrinol. Diabetes* **2017**, *125*, 98–105. [[CrossRef](#)] [[PubMed](#)]
43. Russo, I.; Luciani, A.; De Cicco, P.; Troncone, E.; Ciacci, C. Butyrate attenuates lipopolysaccharide-induced inflammation in intestinal cells and Crohn’s mucosa through modulation of antioxidant defense machinery. *PLoS ONE* **2012**, *7*, e32841. [[CrossRef](#)]
44. Zapolska-Downar, D.; Siennicka, A.; Kaczmarczyk, M.; Kołodziej, B.; Naruszewicz, M. Butyrate inhibits cytokine-induced VCAM-1 and ICAM-1 expression in cultured endothelial cells: The role of NF-kappaB and PPARalpha. *J. Nutr. Biochem.* **2004**, *15*, 220–228. [[CrossRef](#)] [[PubMed](#)]
45. Takigawa, S.; Sugano, N.; Ochiai, K.; Arai, N.; Ota, N.; Ito, K. Effects of sodium bicarbonate on butyric acid-induced epithelial cell damage in vitro. *J. Oral Sci* **2008**, *50*, 413–417. [[CrossRef](#)] [[PubMed](#)]
46. Maeda, T.; Towatari, M.; Kosugi, H.; Saito, H. Up-regulation of costimulatory/adhesion molecules by histone deacetylase inhibitors in acute myeloid leukemia cells. *Blood* **2000**, *96*, 3847–3856. [[CrossRef](#)] [[PubMed](#)]
47. Miller, S.J.; Zaloga, G.P.; Hoggatt, A.M.; Labarrere, C.; Faulk, W.P. Short-chain fatty acids modulate gene expression for vascular endothelial cell adhesion molecules. *Nutrition* **2005**, *21*, 740–748. [[CrossRef](#)]

48. Ogawa, H.; Rafiee, P.; Fisher, P.J.; Johnson, N.A.; Otterson, M.F.; Binion, D.G. Butyrate modulates gene and protein expression in human intestinal endothelial cells. *Biochem. Biophys. Res. Commun* **2003**, *309*, 512–519. [[CrossRef](#)]
49. Vallabhapurapu, S.; Karin, M. Regulation and function of NF-kappaB transcription factors in the immune system. *Annu. Rev. Immunol.* **2009**, *27*, 693–733. [[CrossRef](#)]
50. Magrin, G.L.; Di Summa, F.; Strauss, F.J.; Panahipour, L.; Mildner, M.; Benfatti, C.A.M.; Gruber, R. *10 mM of Butyrate Caused a 4-Fold Increase of  $\beta$ -arrestins-2*; Department of Oral Biology, School of Dentistry, Medical University of Vienna: Vienna, Austria, 2020; Unpublished work.
51. Gao, H.; Sun, Y.; Wu, Y.; Luan, B.; Wang, Y.; Qu, B.; Pei, G. Identification of beta-arrestin2 as a G protein-coupled receptor-stimulated regulator of NF-kappaB pathways. *Mol. Cell* **2004**, *14*, 303–317. [[CrossRef](#)]
52. Lee, S.U.; In, H.J.; Kwon, M.S.; Park, B.O.; Jo, M.; Kim, M.O.; Cho, S.; Lee, S.; Lee, H.J.; Kwak, Y.S.; et al. beta-Arrestin 2 mediates G protein-coupled receptor 43 signals to nuclear factor-kappaB. *Biol. Pharm. Bull.* **2013**, *36*, 1754–1759. [[CrossRef](#)] [[PubMed](#)]
53. Magrin, G.L.; Di Summa, F.; Strauss, F.J.; Panahipour, L.; Mildner, M.; Benfatti, C.A.M.; Gruber, R. *Three Hours Pre-exposure of HSC-2 Cells with Butyrate Could not Reduce the  $IL1\beta$  and  $TNF\alpha$ -induced Increase of ICAM-1, Suggesting that It Requires the 24 h Exposure to Exert the Effects of Butyrate on ICAM-1 Expression*; Department of Oral Biology, School of Dentistry, Medical University of Vienna: Vienna, Austria, 2020; Unpublished work.
54. Lin, H.V.; Frassetto, A.; Kowalik, E.J., Jr.; Nawrocki, A.R.; Lu, M.M.; Kosinski, J.R.; Hubert, J.A.; Szeto, D.; Yao, X.; Forrest, G.; et al. Butyrate and propionate protect against diet-induced obesity and regulate gut hormones via free fatty acid receptor 3-independent mechanisms. *PLoS ONE* **2012**, *7*, e35240. [[CrossRef](#)] [[PubMed](#)]
55. Ledebur, H.C.; Parks, T.P. Transcriptional regulation of the intercellular adhesion molecule-1 gene by inflammatory cytokines in human endothelial cells. Essential roles of a variant NF-kappa B site and p65 homodimers. *J. Biol. Chem.* **1995**, *270*, 933–943. [[CrossRef](#)] [[PubMed](#)]
56. Dong, W.; Jia, Y.; Liu, X.; Zhang, H.; Li, T.; Huang, W.; Chen, X.; Wang, F.; Sun, W.; Wu, H. Sodium butyrate activates NRF2 to ameliorate diabetic nephropathy possibly via inhibition of HDAC. *J. Endocrinol.* **2017**, *232*, 71–83. [[CrossRef](#)] [[PubMed](#)]
57. Chen, X.; Su, W.; Wan, T.; Yu, J.; Zhu, W.; Tang, F.; Liu, G.; Olsen, N.; Liang, D.; Zheng, S.G. Sodium butyrate regulates Th17/Treg cell balance to ameliorate uveitis via the Nrf2/HO-1 pathway. *Biochem. Pharmacol.* **2017**, *142*, 111–119. [[CrossRef](#)]
58. Sun, B.; Jia, Y.; Yang, S.; Zhao, N.; Hu, Y.; Hong, J.; Gao, S.; Zhao, R. Sodium butyrate protects against high-fat diet-induced oxidative stress in rat liver by promoting expression of nuclear factor E2-related factor 2. *Br. J. Nutr.* **2019**, *122*, 400–410. [[CrossRef](#)]
59. Liu, J.; Chang, G.; Huang, J.; Wang, Y.; Ma, N.; Roy, A.C.; Shen, X. Sodium Butyrate Inhibits the Inflammation of Lipopolysaccharide-Induced Acute Lung Injury in Mice by Regulating the Toll-Like Receptor 4/Nuclear Factor kappaB Signaling Pathway. *J. Agric. Food Chem.* **2019**, *67*, 1674–1682. [[CrossRef](#)]
60. Seo, Y.; Park, J.; Choi, W.; Ju Son, D.; Sung Kim, Y.; Kim, M.K.; Yoon, B.E.; Pyee, J.; Tae Hong, J.; Go, Y.M.; et al. Antiatherogenic Effect of Resveratrol Attributed to Decreased Expression of ICAM-1 (Intercellular Adhesion Molecule-1). *Arter. Thromb. Vasc Biol.* **2019**, *39*, 675–684. [[CrossRef](#)]
61. Youn, G.S.; Kwon, D.J.; Ju, S.M.; Choi, S.Y.; Park, J. Curcumin ameliorates TNF-alpha-induced ICAM-1 expression and subsequent THP-1 adhesiveness via the induction of heme oxygenase-1 in the HaCaT cells. *BMB Rep.* **2013**, *46*, 410–415. [[CrossRef](#)]
62. Seo, W.Y.; Ju, S.M.; Song, H.Y.; Goh, A.R.; Jun, J.G.; Kang, Y.H.; Choi, S.Y.; Park, J. Celastrol suppresses IFN-gamma-induced ICAM-1 expression and subsequent monocyte adhesiveness via the induction of heme oxygenase-1 in the HaCaT cells. *Biochem. Biophys. Res. Commun.* **2010**, *398*, 140–145. [[CrossRef](#)]
63. Mole, N.; Kennel-de March, A.; Martin, G.; Miller, N.; Bene, M.C.; Faure, G.C. High levels of soluble intercellular adhesion molecule-1 (ICAM-1) in crevicular fluid of periodontitis patients with plaque. *J. Clin. Periodontol.* **1998**, *25*, 754–758. [[CrossRef](#)]
64. Xu, H.; Gonzalo, J.A.; St Pierre, Y.; Williams, I.R.; Kupper, T.S.; Cotran, R.S.; Springer, T.A.; Gutierrez-Ramos, J.C. Leukocytosis and resistance to septic shock in intercellular adhesion molecule 1-deficient mice. *J. Exp. Med.* **1994**, *180*, 95–109. [[CrossRef](#)] [[PubMed](#)]
65. Yang, M.; Liu, J.; Piao, C.; Shao, J.; Du, J. ICAM-1 suppresses tumor metastasis by inhibiting macrophage M2 polarization through blockade of efferocytosis. *Cell Death Dis.* **2015**, *6*, e1780. [[CrossRef](#)] [[PubMed](#)]

66. Gu, W.; Yao, L.; Li, L.; Zhang, J.; Place, A.T.; Minshall, R.D.; Liu, G. ICAM-1 regulates macrophage polarization by suppressing MCP-1 expression via miR-124 upregulation. *Oncotarget* **2017**, *8*, 111882–111901. [[CrossRef](#)] [[PubMed](#)]
67. den Besten, G.; van Eunen, K.; Groen, A.K.; Venema, K.; Reijngoud, D.J.; Bakker, B.M. The role of short-chain fatty acids in the interplay between diet, gut microbiota, and host energy metabolism. *J. Lipid Res.* **2013**, *54*, 2325–2340. [[CrossRef](#)]
68. Woelber, J.P.; Bremer, K.; Vach, K.; Konig, D.; Hellwig, E.; Ratka-Kruger, P.; Al-Ahmad, A.; Tennert, C. An oral health optimized diet can reduce gingival and periodontal inflammation in humans—a randomized controlled pilot study. *BMC Oral Health* **2016**, *17*, 28. [[CrossRef](#)]
69. Woelber, J.P.; Gartner, M.; Breuninger, L.; Anderson, A.; Konig, D.; Hellwig, E.; Al-Ahmad, A.; Vach, K.; Dotsch, A.; Ratka-Kruger, P.; et al. The influence of an anti-inflammatory diet on gingivitis. A randomized controlled trial. *J. Clin. Periodontol.* **2019**. [[CrossRef](#)]
70. Gruber, R. Osteoimmunology: Inflammatory osteolysis and regeneration of the alveolar bone. *J. Clin. Periodontol.* **2019**, *46 Suppl 21*, 52–69. [[CrossRef](#)]
71. Tang, C.; Ahmed, K.; Gille, A.; Lu, S.; Grone, H.J.; Tunaru, S.; Offermanns, S. Loss of FFA2 and FFA3 increases insulin secretion and improves glucose tolerance in type 2 diabetes. *Nat. Med.* **2015**, *21*, 173–177. [[CrossRef](#)]
72. Cantley, M.D.; Zannettino, A.C.W.; Bartold, P.M.; Fairlie, D.P.; Haynes, D.R. Histone deacetylases (HDAC) in physiological and pathological bone remodelling. *Bone* **2017**, *95*, 162–174. [[CrossRef](#)]
73. Huynh, N.C.; Everts, V.; Ampornaramveth, R.S. Histone deacetylases and their roles in mineralized tissue regeneration. *Bone Rep.* **2017**, *7*, 33–40. [[CrossRef](#)] [[PubMed](#)]
74. Pourgonabadi, S.; Muller, H.D.; Mendes, J.R.; Gruber, R. Saliva initiates the formation of pro-inflammatory macrophages in vitro. *Arch. Oral Biol* **2017**, *73*, 295–301. [[CrossRef](#)] [[PubMed](#)]



© 2020 by the authors. Licensee MDPI, Basel, Switzerland. This article is an open access article distributed under the terms and conditions of the Creative Commons Attribution (CC BY) license (<http://creativecommons.org/licenses/by/4.0/>).